Archives of Civil and Mechanical Engineering (2023) 23:116
https://doi.org/10.1007/s43452-023-00662-2

ORIGINAL ARTICLE

Effect of alkaline treatment on mechanical properties of palmyra and S-glass fiber reinforced epoxy nanocomposites

Navuluri Padma Sravya[1] · S. Sivaganesan[1] · R. Venkatesh[2] · R. Manikandan[2]

Received: 18 January 2023 / Revised: 29 March 2023 / Accepted: 2 April 2023 / Published online: 13 April 2023

Abstract

Although epoxy resins have many advantages, their use needs to be expanded by improving their mechanical properties, including a wide variety of material quality, easy processing, negligible shrinkage due to curing, and good adhesiveness to many forms of fiber materials. The research focuses cost-effective utilization of palmyra fiber treated with 5% alkali solution and different volume percentages of S-glass fiberglass incorporated by epoxy resin developed by hand layup technique. The final epoxy hybrid composite consists of different weight ratios of palmyra/S-glass fiberglass as 25:75, 50:50, and 75:25. Influences of palmyra (treated) fiber dispersion quality on density, voids, mechanical and moisture absorption performance of the epoxy hybrid composite is studied by ASTM rule. The elevated output characteristics performance is compared with untreated fiber composite. Based on the rule of mixture, composite density is varied and Archimedes' principle measures voids. The alkali treated composite samples showed good tensile stress, flexural and impact strength. While compared to untreated fiber composite, the tensile, flexural, and compressive strength of TPF/GF(25:75) composite was improved by 19.58%, 29%, and 14.3%, respectively. The reduced water absorption behaviour was observed on the treated composites. The effect of fiber dispersion on the mechanical failure of hybrid composite is studied by SEM analysis.

Keywords Alkaline treatment · Palmyra fiber and glass fiber · Hybrid nanomaterial · SEM · Water adsorption studies

1 Introduction

Natural fibers as reinforcement nanocomposites are developed in different industries, including marine structures, supporting structures, automobile components, and aviation, which are subjected to various forces and stresses. To replace traditional metal components and synthetic composite materials, many scientists are actively experimenting by using various fibers and resins to create essential parts for advanced and complex parts [1]. Numerous studies on fiber composites have recently focused on the characteristics of glass fiber [2]. Therefore, researchers seek environmentally acceptable alternatives and maximize hybrid performance by incorporating natural fibers to replace or reduce synthetic fabrics. The distinct qualities of natural fibers include their superior physical strength, excellent heat transfer characteristics, low density, good acoustic properties, and biodegradability [3]. Organic fibers, including jute, kenaf, papaya, sisal, and palm, have received increasing attention due to their high interfacial adhesion for establishing organic polymeric materials. [4]. Additionally, extensive investigation is aimed at the compatibility of resin composites with various organic polymers continued in this field. The fibers are mixed with different lengths and physically tested using different matrix materials to achieve the maximum stiffness of the FRC material [5].

Due to essential properties such as adhesion, heat resistance, excellent biocompatibility, and thermal properties, epoxy resins have emerged as a widely used resource over the past several decades. However, these technologies have

✉ Navuluri Padma Sravya
navuluri.sravyaa@gmail.com

✉ R. Venkatesh
venkidsec@gmail.com

S. Sivaganesan
sivaganesanse@gmail.com

R. Manikandan
mani131990@gmail.com

[1] Department of Mechanical Engineering, School of Engineering, Vels Institute of Science Technology and Advanced Studies, Chennai 600117, Tamilnadu, India

[2] Department of Mechanical Engineering, Saveetha School of Engineering, SIMATS, Chennai 602105, Tamilnadu, India

seen significant progress and improvement over the past 20 years, which are significant today [6]. Recent research has focused on forming epoxy resin composites, although previously excellent resins have significantly been strengthened by using and modifying them as composite matrixes. Among the most versatile thermoplastic groups, epoxy resins are used in painting and surface coating, composite materials, wind turbines, buildings, and electrical systems [7, 8]. Due to their unique qualities, including strength properties, chemical stability, high thermal stability, and heat transfer adaptability, epoxy resins have been used in many industries over the past century [6]. Epoxy resins-based composites are the most significant materials in thermosetting groups for the applications of building, wind energy, composites, electrical, and coatings [9, 10]. Epoxies are often hardened and combined with an organic solvent to solidify wet mixtures. The epoxy resin becomes a more durable, long-lasting liquid when a curing agent is added. [11, 12]. Because previously special polymers have been greatly strengthened by using materials for customization and as a composite matrix, researchers are currently focusing on improving epoxy resin compositions [13].

Natural fiber-reinforced polymer matrix composite was developed by conventional technique and the effect of chemically treated natural fiber on water absorption properties was studied experimentally. The investigational results are compared with untreated fiber. The treated fiber offered less moisture absorption than untreated fiber [14]. Epoxy-based polymer composites' flexural characteristics are studied with and without nano clay. The nanoclay facilitates good flexural response compared to conventional epoxy resin [15]. However, the properties of the composite are decided by weathering process [16]. The polyester and plastic/ rubber composite is synthesized via 549 and 550 Napier composite and studied its effects on the compressive strength of composite [17]. Vacuum transfer molding developed glass fiber reinforced plastic/aluminum laminate hybrid composite tensile and flexural strength is investigated by ASTM standards and found glass fiber offered good tensile and flexural strength compared to base laminate [18]. Natural cellulosic fiber gained great potential in polymer matrix composite fabrication due to its superior stiffness, easy availability, and low cost [19]. The polymer-based hybrid composite is prepared by utilizing different weight percentages of palmyra fiber bonded with glass fiber and its effects on mechanical properties and moisture absorption were studied and the results are compared with different fiber length mat composites.

The functional palmyra is performed enhanced mechanical and moisture behaviour [20]. Poly (lactic acid) hybrid composite is synthesized using Alkali treated sugar palm and glass fiber for motorcycle applications. Developed composites' mechanical and flammable behaviour are studied and compared with conventional Acrylonitrile Butadiene Styrene plastics. It performed higher hardness and impact strength of 88.6 HRS and 3.10 kJ/m^2 [21]. Recently, the mechanical properties of inset with sisal fiber (Alkali treated) ASTM standards and its experimental findings study reinforced polymer matrix hybrid composite are compared to untreated fiber reinforced polymer composite.

The results showed that the 5% alkali-treated composite tensile, flexural, and impact strength was increased by 5.21, 9.25, and 5.98 [22]. However, the thin wall graphene nanoplatelets bonded composite post-yield region is the strength by vibration technique and the yield stage was found using the hyperbolic differential quadrature method [23]. Functionally grade CNT fiber-embedded polymeric nanocomposite layers were analyzed by porosity-dependent vibration technique and considered for hygrothermal effect [24]. Compressive strength of nano silica-reinforced concrete via machine learning technique [25]. Integral higher-order shear deformation theory adopted non-linear cylinder bending analysis of single-walled carbon nanotubes was estimated their functionality and the micro thickness direction was measured by micromechanical method [26]. Carbon nanotube-reinforced polymeric composite was developed for doubly curved micro-shell panel applications. The composite's mechanical behaviour is studied with the deformation theory of shear in a curvilinear coordinate system mixed with the approach of the non-classical system [27]. The effect of non-linear functionality grade CNT fiber on the mechanical properties of composite is experimentally studied for beam applications [28].

Similarly, free vibration study is made [29], dynamic analysis of SW-CNT is studied [30]. The computational framework adopted for sandwich doubly curved nanocomposite panels [31]. Frequency simulation system to be adopted for imperfect honeycomb core sandwich disk with multiscale hybrid nanocomposite [32]. Framework base sandwich disk composite was proposed with higher order mechanics [33], vibration analysis [34], and stress and strain response with three-dimensional analysis [35].

The present study aims to enhance the epoxy matrix's mechanical characteristics and water absorption behaviour by adding (different ratios) alkali treated Palmyra and S glass fiber synthesized through a cost-effective hand layup route. The effect of material dispersion on epoxy composite mechanical failure is analyzed using scanning electron microscope (SEM). According to ASTM standards, the tensile, compressive and flexural strength is measured by INSTRON 3382' universal tensile testing machine. Archimedes' principle evaluates the density and voids of composites. The water absorption test was carried out with different (treated) fiber lengths of 2, 4, and 6 mm, producing epoxy composite for 7 days. Based on an integrated design process in the future, polymer composites to be fabricated based on optimized parameters such as fiber length, material types, treatment methods, and volume fraction.

2 Materials and methods

Epoxy is a conventional name for the epoxide structural group and the essential features of epoxy resins or cured finished products. Prepolymers and polymers are major responsive elements of epoxy resins, also called polyepoxides. Through catalytic photopolymerization, epoxy resins can interact (cross-link) with themselves or with a wide range of co-reactants such as reactive functional groups, amines, protons (including acid anhydrides), phenolic compounds, ethyl alcohol, and oxidizing agents. These co-reactions are named hardeners, and the cross-linking response is classified as a curing process. The thermosetting polymers are formed by polyfunctional hardeners or reactions of polyepoxides, often developing the physical, thermal, and wear behaviour of epoxy composites.

This present research uses the palmyra fiber (LY-556) extracted from leaf sheets of the Palmyra Palm and is produced in southern and eastern India. The use of fruit bunch waste in oil palm can reduce the amount of enzyme production compared to alternative sources. The advantages of palm oil fruit bunch fibers include accessibility, biodegradability, ease of fabrication, and high strength. This type of fiber has low viscosity, dimensional stability, high material strength, and corrosion resistance when the hardener Aradur HY-951 is added as a matrix material. Tables 1 and 2 show the mechanical properties of epoxy resin and palmyra fiber.

2.1 Fiber treatment

Manufactured fiber reinforcement is alkali-treated for fibers of three different weights and lengths. All three fiber types were subjected to several treatment periods with 5% NaOH solvent. The alkaline treatment process was conducted for three different length fibers of 2, 4, and 6 cm in epoxy composites. The chemicalized treatment removes contaminants from the fiber material and ensures molecular orientation. During the alkali treatment, the fibers are thoroughly cleaned with distilled water and then dried at ambient temperature for one day. The fibers were separated into smaller fibers of 2, 4, and 6 cm lengths to fabricate the nanocomposite. This is done by wetting the fiber with the polymer matrix properly and it has better strength than untreated fibers.

Table 1 Epoxy resin physical properties

Properties	Unit	Value
Density	kg/cm^3	1200
Tensile strength	MPa	70
Equivalent epoxy weight	g/eq	187
Viscosity at room temperature	cp	12, 600
Appearance	–	Light yellow
Modulus of elasticity	GPa	20

Table 2 Properties of Palmyra fiber

Properties	Unit	Values	
		Treated	Untreated
Density	g/cm^3	1.30	0.456
Modulus of elasticity	GPa	2.5–5.4	3.24
Tensile strength	MPa	97–196	120
% Of elongation	–	2–4.5	3.26
Lignin content (%)	–	21.2	13.48
Cellulous content (%)	–	49.6	58.8
Hemicelluloses (%)	–	18	22.8

2.2 Polymer composites fabrication

Hand lay-up is the most popular technique for fabricating polymer composite materials during manufacturing. Using this process, the fiber pieces were reduced to the desired size. The polymer was processed to a dimension of 80 × 30 × 5 mm using a spray-coated mold. A mixture of resin and hardener was placed onto the fiber in stages using a hand lay-up method, and successive layers of fiber were poured over the surrounding matrix to create the desired thicknesses. The samples were heated for 5 min at 150 °C under 2.5 MPa of axial pressure. The detailed fabrication process and their testing samples are shown in Fig. 1. The formation of epoxy composites with their percentage of mixed proportions is shown in Table 3.

3 Mechanical testing

3.1 Density measurement

The physical properties of composite samples, including density, water absorption, and void content, were evaluated according to ASTM standards. Experimental density was calculated for the proposed hybrid polymer composites according to ASTM D792. A digital vernier caliper with a precision of 10^{-2} mm was used to measure the sample dimensions, while an electronic balance of 10^{-4} kg was used to measure the volume of the samples. The experimental and theoretical densities are calculated according to the composition law for the mathematical expression in Eqs. (1) and (2).

$$\rho_{\exp} = \frac{\text{Mass}}{\text{Volume}} \tag{1}$$

Fig. 1 Details fabrication layout and its test samples

Table 3 Formation of epoxy-based composites

The mixing ratio of reinforcements	Designation	Volume ratio (Epoxy:palmyra:glass fiber)			Fiber treatment
		Epoxy resin	Palmyra	Glass fiber	
GF (100%)	GF	1	0	1	Untreated
PF (100%)	UTPF	1	1	0	Untreated
EP + 25% PF + 75% GF	UTPF/GF (25:75)	1	0.25	0.75	Untreated
EP + 50% PF + 50% GF	UTPF/GF (50:50)	1	0.5	0.5	Untreated
EP + 75% PF + 25% GF	UTPF/GF (75:25)	1	0.75	0.25	Untreated
PF (100%)	TPF	1	1	0	Alkali treated
EP + 25% PF + 75% GF	TPF/GF (25:75)	1	0.25	0.75	Alkali treated
EP + 50% PF + 50% GF	TPF/GF (50:50)	1	0.5	0.5	Alkali treated
EP + 75% PF + 25% GF	TPF/GF (75:25)	1	0.75	0.25	Alkali treated

$$\rho_{th} = \rho_{PA}V_{PA} + \rho_G V_G + \rho_m(1 - V_{PA} + V_G) \quad (2)$$

where ρ_m, ρ_m, ρ_m, density of matrix, Palmyra and glass fiber; V_{PA} and V_G volume fractions of Palmyra and glass fiber.

Also, the void content prepared composites are calculated by following expressions

$$\text{Void content}(\%) = \frac{\rho_{th} - \rho_{exp}}{\rho_{th}} \times 100 \quad (3)$$

3.2 Water adsorption

The water absorption percentage of hybrid composites is measured over a wide range at room temperature. The prepared polymer composites of initial weight were noted before being submerged in deionized water. The confidence interval for the test conducted following ASTM D570-98 appears to be 60 × 10 × 4 mm. The composite specimens were removed from the water after 24 h and the samples were weighed. The percentage of water adsorption is determined using the following mathematical expression

$$\%\ \text{of water absorption} = \frac{w_f - w_i}{w_i} \times 100 \quad (4)$$

where w_f, w_i final and initial weight of the specimen

3.3 Tensile, flexural and compressive test

The UTM cross-head speed of 2 mm/min was carried out for tensile strength and specimens were dimensioned (300 × 30 × 3) as per ASTM D3039 standards. Three specimens of tensile strength average values are taken from each proportion of polymer composites. TM conducted flexural properties with 5 kN load cell, strain rate 0.01 mm/mm/min, cross-head speed-2.56 mm/min on three-point testing according to ASTM D-790-10 and the temperature range 23 ± 1 °C at relative values humidity of 50 ± 5%. Three samples of average values are taken for the standard specimen dimension is 150 × 23 × 6 mm. Similarly, INSTRON 3382's was tested for compressive strength using a 100 kN load cell following ASTM D695-15 standards. The standard dimension of 12.5 × 6 mm of three specimens was extracted from each prepared polymer composite. The interfacial bonding between fiber/matrix reinforcement and fracture surface was characterized after mechanical testing. Experiments were performed using a Quantum Superpositions 200 model with an operating distance of 9.8–12.3 mm and an accelerating voltage of 15 kV. The degraded fiber surface was treated to allow efficient electronic conductivity in the hybrid. The mechanical tensile, flexural and compression test sample fixed with the test machine is shown in Fig. 2.

4 Results and discussions

4.1 Density and void content

The prepared palmyra fiber reinforced composites of experimental densities (ρ_e) agree with the theoretical density (ρ_t). Table 4 shows the fiber reinforcement on epoxy nanocomposites of measured and calculated density and void fraction. A minor difference has been observed due to void content during the material processing. Adding glass fiber to the composite material has resulted in significant improvement in density, as predicted because glass fiber is denser than polyamide fiber.

The amount of void space and porosity present during the processing of fiber-reinforced resin polymer composites is used to calculate void content. The effect of void formation reduces the strength of the matrix because increasing the void content increases the porosity level. Table 4 noted that theoretically, estimated densities are not equal to experimentally observed densities. Increasing glass fiber (25%, 50%, and 75%) in epoxy composites conduct to increase in theoretical and experimental density. The hand layup process achieves good fiber saturation and produces hybrids with minimum void content (less than 5%). Beyond 75% GF filler content, the test density of composite materials may not be

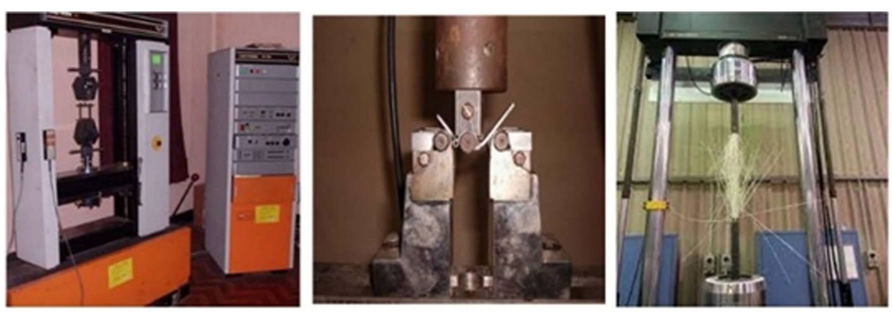

Fig. 2 Test sample fixed with test equipment

Table 4 Experimental density and theoretical density

S. no	Composite preparation	Theoretical density(ρ_t) g/cm^3	Experimental density (ρ_e) g/cm^3	Void fraction $\Delta v = \frac{\rho_t - \rho_e}{\rho_t}$
1	GF (100%)	1.285	1.258	2.10
2	PF (100%)	1.108	1.078	2.70
3	EP + 75% PF + 25% GF (treated)	1.366	1.345	1.53
4	EP + 50% PF + 50% GF(treated)	1.428	1.396	2.24
5	EP + 25% PF + 75% GF (treated)	1.474	1.422	3.52
6	PF (100%)	1.095	1.056	3.56
7	EP + 75% PF + 25% GF (untreated)	1.385	1.343	3.03
8	EP + 50% PF + 50% GF (untreated)	1.405	1.375	2.13
9	EP + 25% PF + 75% GF (untreated)	1.450	1.412	2.62

further reduced. Thomason et al. observed the same results when the fiber/filler concentration exceeded the optimum level. The physical properties of the composite materials automatically decreased. The palmyra fiber obtained a maximum void fraction of 3.56% for unreinforced epoxy composites, whereas a lower void fraction was obtained for EP + 25% PF + 75% GF epoxy composites. It increases the test density of 25%, 50%, and 75% GF while reducing the void area when combined with palmyra and GF reinforcement and resin.

4.2 Water absorption test

Dimensional instability, cracking and low strength of fiber-reinforced epoxy composites are analyzed based on water absorption. As a result of water adsorption with different volume fractions concerning different fiber lengths for treated fiber as shown in Table 5. A high-precision weighing and balancing machine estimated and considered the initial weight of the sample during the water absorption test. After that, the samples were placed in fresh water and their mass was recorded as the final mass of composite specimens. This test was conducted for 7 days. Due to cellulose and naturally hydrophilic chemical composition, natural fibers are susceptible to water absorption. As the cellulose content rises due to the increase in the amount of free hydrophilic segments in the fiber, the water absorption of the produced fiber will probably increase. From the experimental results, the water absorption range of prepared mixtures is obtained from 0.08% to 0.5%.

4.3 Mechanical properties

4.3.1 Tensile strength

A comparison between the before and after tensile tests of all prepared samples is shown in Fig. 3, and the tensile strength of treated and untreated epoxy-palmyra fiber was tested. The TS of epoxy-reinforced nanocomposites is increased with an increase in PF and GF compositions [14]. The tensile strength of alkali-treated epoxy-fiber reinforced composites was 70.64 MPa, higher than untreated and palmyra fiber-reinforced composites. The GF (100%) has shown that the tensile strength is 58.62 MPa, less than that of hybrid polymer nanocomposites(Table 6). The treated fiber-reinforced composite (UTSC) showed a higher value than the epoxy composite without fiber reinforcement. It demonstrates the crucial role of palmyra fiber reinforcement in enhancing the

Table 5 Water adsorption for different volume fractions (treated)

Fiber size	Volume fractions of fiber	Initial weight	Final weight	Percentage of absorption
2	EP + 75% PF + 25% GF	4.121	7.442	80.5
	EP + 50% PF + 50% GF	5.122	7.010	36.86
	EP + 25% PF + 75% GF	5.455	7.624	29.76
4	EP + 75% PF + 25% GF	5.226	7.132	36.47
	EP + 50% PF + 50% GF	4.956	6.854	38.29
	EP + 25% PF + 75% GF	4.772	6.854	43.62
6	EP + 75% PF + 25% GF	4.152	6.442	55.15
	EP + 50% PF + 50% GF	5.236	6.325	20.80
	EP + 25% PF + 75% GF	5.324	7.524	41.32

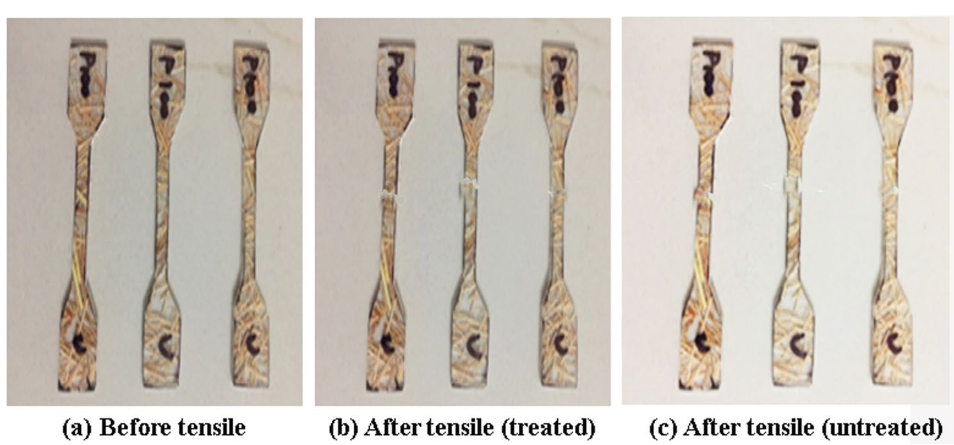

Fig. 3 Schematic representation of before and after tensile test specimens for both treated and untreated specimens (ASTM D3039)

Table 6 Tensile strength and stress value of epoxy composites with palmyra and Glass fiber reinforcement

Percentage of reinforcements	Tensile strength (MPa)		Stress (MPa)	
	Untreated	Treated	Untreated	Treated
GF (100%)	58.62	–	46.58	–
PF (100%)	33.52	39.65	29.34	33.24
EP+75% PF+25% GF	42.51	52.31	38.48	41.26
EP+50% PF+50% GF	42.51	55.68	34.25	45.32
EP+25% PF+75% GF	52.14	62.35	47.12	53.76

specimen's tensile strength. The alkali-treated palm rind-treated reinforced composite (TPF) showed a tensile strength value of 30 MPa and the calculated value seems to be almost 80% higher than the untreated composite. The results of all tests revealed that in terms of tensile strength, the treated palmyra fiber-reinforced nanocomposite was superior to the untreated fiber-reinforced composite.

Epoxy with palmyra FRC showed a tensile strength of 42.51 and 52.31 MPa, which was very low compared to other combinations of composites. Comparatively, composites reinforced with 25% palmyra fiber and 75% S-glass fiber had a higher tensile strength of 60.25 MPa than composites without adding palmyra fiber and glass fiber reinforcement, as shown in Fig. 4. All the test results showed that the treated palm fiber-reinforced epoxy composite surpassed the untreated fiber-reinforced composite in terms of performance. The stress–strain behaviour of hybrid epoxy composites was recorded during the tensile test, as shown in Fig. 5.

The values of tensile strength stress value increased to 35–42% due to expansion before fiber content decreased during the treatment process. According to the test results, the

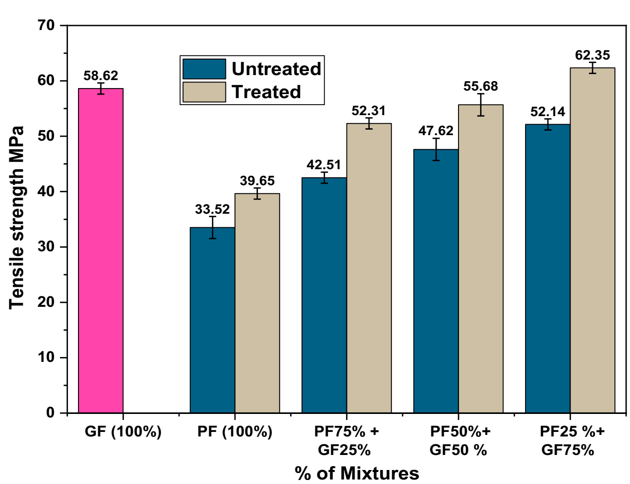

Fig. 4 Glass-fiber/palm-fiber reinforced composites of tensile strength for treated and untreated

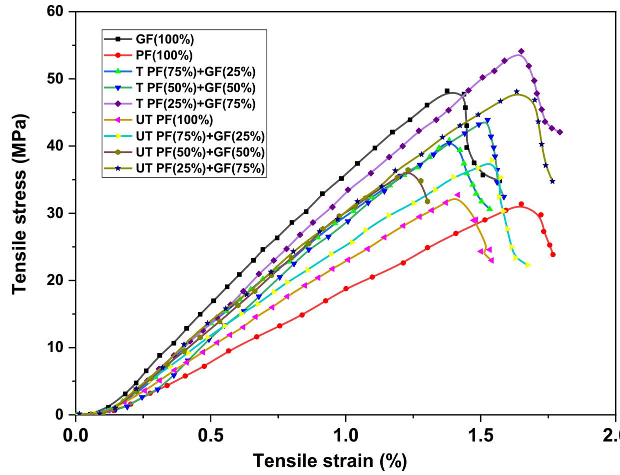

Fig. 5 Tensile stress–strain curve of epoxy-reinforced hybrid composites

tensile strength of the prepared materials decreased up to 50 (PF):50 (GF) wt%, before there was a modest improvement of up to 68% for composites including treated fiber composites. Due to the integration of fiber waste, there was no increase in tensile strength. The critical size, below which the material does not reinforce the matrix, is the smallest size of fiber. Larger stresses develop at moderate strains and the stress concentration is not uniform when there are not enough fibers to control the properties of the matrix. However, once the minimum number of fibers required to constrain the matrix is reached, the stress distribution becomes uniform and the fibers begin to reinforce the matrix. The same trend was observed for using natural rubber composites by Hasan et al. [36]. On the other hand, the size of fiber 20–100 mm may be the reason for achieving low strength for untreated and treated fiber polymer composites. Very short fiber stress never reaches the fracture point, and its only function is to prevent matrix crack propagation. The failure may be occurred by using a large type of fiber. When a fiber cracks, the growing microcrack can no longer be properly intercepted, which reduces the fiber's toughness.

4.3.2 Flexural strength

Figure 6 displays the treated palmyra and glass fiber reinforced epoxy composites' flexural strength of epoxy hybrid composites. Variations in flexural stress–strain behaviour were observed due to different proportions of reinforcement. According to Hook's law, the stress is directly proportional to strain for the observed treated and untreated polymer nanocomposite behaviour [15]. The curves show that all composites failed after initial cracking due to their elastic deformation. The effect of concentrations on untreated

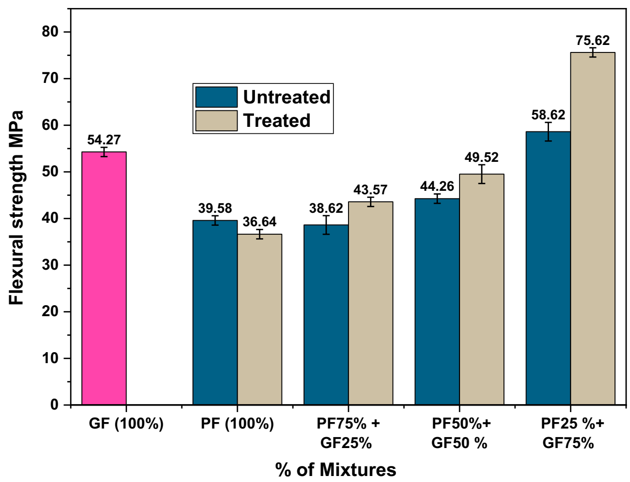

Fig. 6 Flexural strength of epoxy composites with different volume fractions of palmyra (PF) and Glass fiber (GF) reinforcement

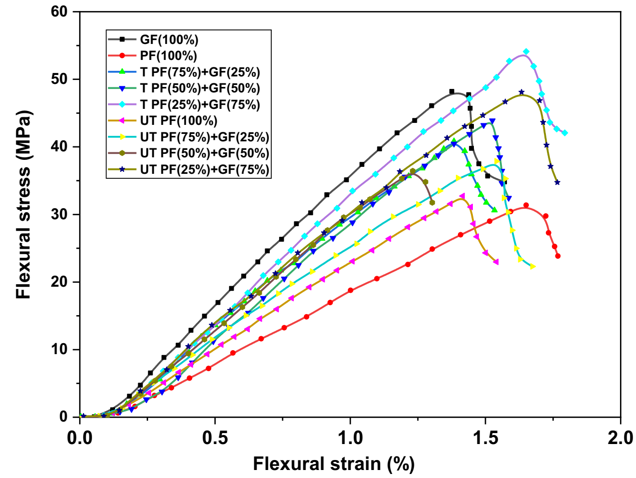

Fig. 7 Flexural stress–strain curve of epoxy composites with different volume fractions of palmyra (PF) and Glass fiber (GF) reinforcement

and treated fibers of flexural strength and flexural stress are shown in Table 7.

It is anticipated that a fracture will start on the tension relatively close to the beam and slowly spread into the longitudinal beam of the structures. According to the composite specimens, there seem to be differences in the flexural stress–strain behaviour, as shown in Fig. 7. The structures display typical polymer composite materials' mechanical and physical properties in a flexural stress–strain pattern.GF was obtained as the maximum flexural stress–strain gradient at 45 MPa, followed by PF25% + GF75% at 52.34 MPa [16]. The alkaline formation in the alkaline group attached to the fiber-reinforced composites leads to the development of the bonding strength between the fiber and matrix. The results demonstrated that alkali treatment improves the flexural and yield strength of Epoxy/Palmyra/Glass fiber reinforced composites.

Figure 6 shows that the increase in hybridization increases the flexural strength from 43.57 to 75.62 MPa. The experimental results reveal a promising increase in flexural properties of PF/GF/epoxy hybrid nanocomposites between untreated hybrid and treated palmyra-reinforced epoxy hybrid nanocomposites [17].

An alkali treatment was applied to palmyra fiber, which benefits the flexural properties of PF/GF/epoxy composites. Additionally, it was discovered that the fiber-to-fiber ratio impacted the qualities and traits of the composites (PF: GF). GF aims to withstand the high load capacity before torsional failures while mixing with PF entirely randomly to improve the high strength and modulus. This may be due to sufficient fiber effectively transferring the stress between the matrix and the reinforcing fibers [18]. Flexural properties are improved with an increase in GF content.

The representation of fractured specimens before and after the flexural test for both treated and untreated epoxy composites is shown in Fig. 8. Figure 9 shows the allowable difference between the maximum flexural load for epoxy/PF/GF hybrid nanocomposites for untreated and treated palmyra fiber-reinforced composites. The flexural load-bearing capacity of PF/GF/epoxy hybrid composites was improved by adding untreated and treated PF [14]. The TPF/GF/epoxy hybrid composites with TPF25% + GF75% fiber-to-fiber ratio had a higher flexural load of 394.52N compared to UT PF25% + GF75% of 384.23N. In addition, the flexural load of TPF (25%): GF (75) was more significant than the 338.2N flexural applied load of pure glass fiber composites. When using the same fiber–fiber ratio for PF/GF/epoxy mixture nanocomposites with PF (75%): GF (25%) fiber–fiber ratio, the maximum flexural load of TPF increases by 10%, especially in contrast to UTPF [20]. Compared to UTSPF, with a relatively similar fiber–fiber ratio for PF/GF/epoxy composite materials with a fiber–fiber ratio of PF (50%): GF (50%), the maximum flexural load of TPF improved by 6%.

The PF outer layer underwent significant transformations due to NaOH alkaline treatment. This increased

Table 7 Flexural strength and stress value of epoxy composites with palmyra and glass fiber reinforcement

Percentage of reinforcements	Flexural strength (MPa)		Flexural stress (MPa)	
	Untreated	Treated	Untreated	Treated
GF (100%)	54.27	–	45.28	–
PF (100%)	39.58	36.64	27.56	32.54
EP + 75% PF + 25% GF	38.62	43.57	24.52	37.58
EP + 50% PF + 50% GF	44.26	49.52	35.75	42.78
EP + 25% PF + 75% GF	58.62	75.62	44.26	52.64

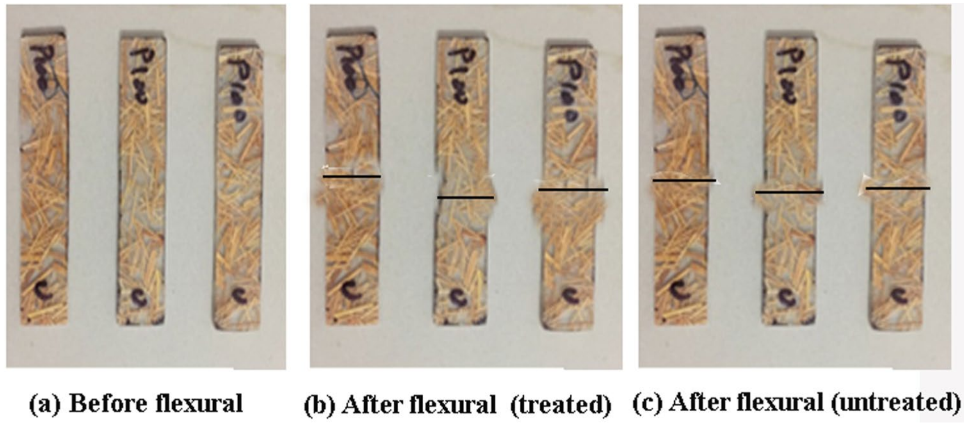

Fig. 8 Schematic representation of before and after flexural test specimens for both treated and untreated specimens (ASTM D-790-10)

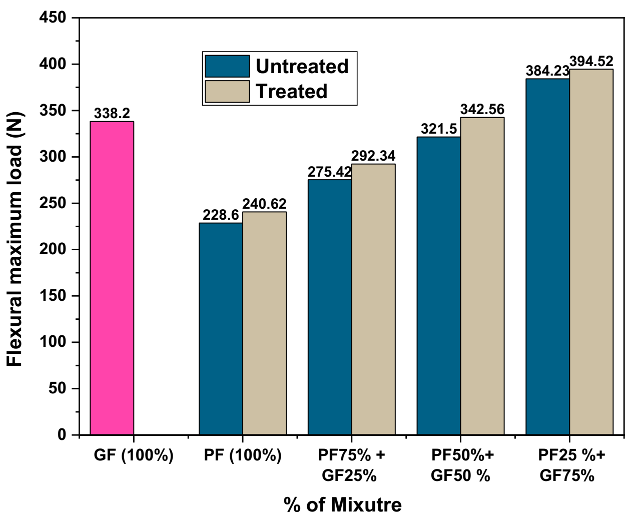

Fig. 9 Flexural test of maximum load for treated and untreated fiber-reinforced epoxy composites

Table 8 Flexural load value of epoxy composites with palmyra and glass fiber reinforcement

Percentage of reinforcements	Flexural max load (N)	
	Untreated	Treated
GF (100%)	338.2	–
PF (100%)	228.6	240.62
EP + 75% PF + 25% GF	275.42	292.34
EP + 50% PF + 50% GF	321.5	342.56
EP + 25% PF + 75% GF	384.23	394.52

epoxy interfacial adhesion at the interaction and continued to improve interfacial interaction and structural interlocking generated by various minor void spaces on the fiber surface [19]. Crosslinking interactions may also result in higher strength for composites treated with NaOH. Evans et al. experimented on fiber-reinforced composites, finding similar trends of alkaline-treated fiber compared to untreated fiber-reinforced epoxy composites. The effect of treated fiber results and comparison with the maximum flexural load during the flexural test are shown in Table 8.

4.3.3 Compressive strength

The compressive test analysis of epoxy composites of the test setup shows in Fig. 10. Compressive test experimental results demonstrate the compressive and stress–strain behaviour of treated and untreated palmyra glass fiber polymer composites samples. Figure 10 shows the compressive

Fig. 10 Compressive strength test of epoxy composites reinforced with palmyra and S-Glass fiber

strength of glass fiber-reinforced epoxy hybrid nanocomposites. Fartini et al. found the compressive strength results and established the non-linear behaviour. A higher value was placed on the factors and variables for compressive yield strength due to the matrix's highly compressed, cracked, and brittle microparticles.

In addition, treated fiber composites were found to have slightly larger values than untreated composites. Figures 11 and 12 make it clear that both treated and untreated composites constructed entirely of SPF perform poorly compared to composites made from hybridizing palmyra and S-glass fiber. However, the treated hybrid epoxy composites have a high compressive strength compared to untreated ones. To substantially dissolve the hydrogen bonds in the cellulose chains, PF is pre-treated with the solution of NaOH. This increases the exterior area of the fiber for more excellent responsiveness to benzoylation. Utilizing benzoylation to reduce palmyra fiber's hydrophilicity increases the compressive properties of epoxy hybridized composites. It makes palmyra fiber more compatible with hydrophobic matrix [37].

On the other hand, a significant impact was observed from the hybridization of palmyra fiber reinforced with glass fiber in epoxy composites. This clearly shows that adding glass fiber gradually increases the compressive properties. Also, due to GF's high strength and high modulus, it is superior to SPF. Analysis of the results also indicated that the amount of fiber-to-fiber content significantly improves the compressive properties of composites. Maximum tensile stress tensile strength that hybrid PF/GF/epoxy composite materials can withstand during global testing. The stress on the specimen surface at failure is measured before the natural fibers fully crack. The higher tensile strength, 64.25 MPa, was obtained for PF25%:GF75% reinforcement on epoxy hybrid nanocomposites, which was higher than that of with and without palmyra fiber reinforced hybrid composites, as observed from

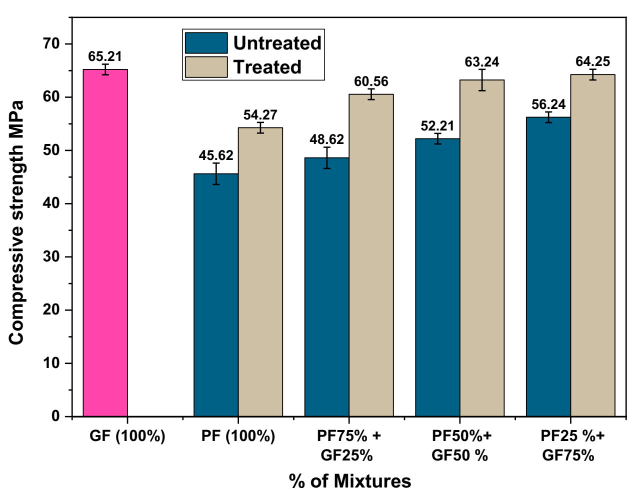

Fig. 11 Compressive strength epoxy composites with different volume fractions of palmyra (PF) and glass fiber (GF) reinforcement

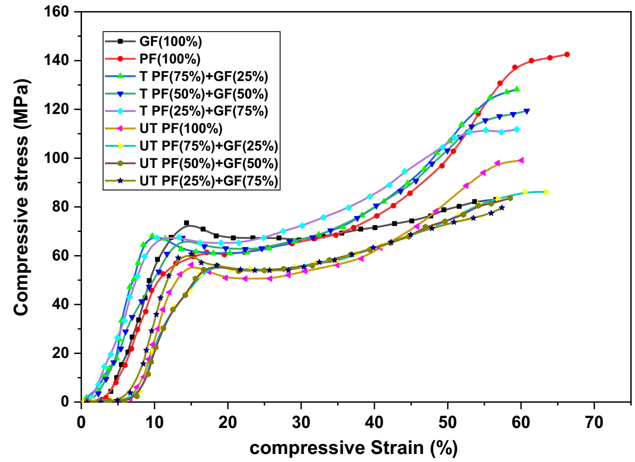

Fig. 12 Compressive stress–strain behaviour epoxy composites with different volume fractions of palmyra (PF) and Glass fiber (GF) reinforcement

Table 9. The compressive strength and stress value obtained from the experimental tests is shown in Table 9.

4.3.4 Compressive stress–strain behaviour

Figure 12 shows the compressive stress–strain behaviour of glass fiber-reinforced epoxy hybrid nanocomposites. The test was conducted by using UTM with a uniform crosshead speed. Figure 12 showed non-linear behaviour and is consistent with previously published research. According to Fig. 12, the curves' compressive strength, compressive failure strain, and concrete strength vary slightly. Although additives impact composite materials' compressive stress, the polymer matrices' stiffness is primarily reflected in the composite's longitudinal strength properties. According to the compressive stress test results, the prepared specimens primarily experience shear-compression type brittle fracture. Usually, shear and densification failure occur at the junction where the load is proposed in composites formed under high stress. Ultimate strength interface failures are observed due to the matrix/fiber. When the fiber exceeds the ultimate

Table 9 Compressive strength and stress value of epoxy composites with palmyra and glass fiber reinforcement

Percentage of reinforcements	Compressive strength (MPa)		Compressive stress(MPa)	
	Untreated	Treated	Untreated	Treated
GF (100%)	65.21		62.34	–
PF (100%)	45.62	54.27	84.62	158.64
EP + 75% PF + 25% GF	48.62	60.56	105.26	122.46
EP + 50% PF + 50% GF	52.21	63.24	75.28	110.26
EP + 25% PF + 75% GF	56.24	64.25	65.26	118.62

compressive stress, it can withstand and may break in shear failure. The second fragment of the uniaxial compressive curve, which appears after the final compressive stress, shows the progression of fiber failure. Deformation failure, local fiber micro-buckling along the elastoplastic matrix, yield rate related to fiber micro-buckling, and actual fiber tensile and flexural failure during uniform compression are common causes of nanocomposite failure.

Figure 12 shows that both treated and untreated composites fully reinforced with PF achieved low strength compared to glass fiber composites. In contrast, pure TSPF composites have higher compressive strength (64.25 MPa) than pure PF composite materials made only from PF (54.25 MPa). The ultimate tensile yield strength of the purely treated palmyra fiber composites is also 52.27 MPa higher than the pure, untreated palmyra fiber composites, as seen in Fig. 12 (42.62 MPa). PF was pre-treated with sodium hydroxide to partially eliminate the formation of hydrogen bonds in the lignocellulose chains. As a result, the surface of the fiber is more alkali-reactive.

The tensile, flexural, and compressive properties are improved by using alkaline to reduce the hydrophilic nature of PF. As a result, the PF and hydrophobic matrix are more uniform. In addition, the hybridization of the PF with the GF should also be considered. Figure 12 shows that adding GF reinforcement to the composite material significantly impacts its compressive yield strength and stress–strain behaviour. The maximum yield strength of epoxy hybrid mixed composites of both treated and untreated composites are shown in Table 10. However, the addition of GF is highly advantageous to palmyra fiber due to GF leads to increases the compressive strength. The analysis of the results also indicates that the amount of fiber-to-fiber composition significantly impacts the improved performance in the compressive and shear properties of the nanocomposites.

4.3.5 SEM analysis

The fiber matrix interfacial bonding strength and fractured surfaces were analyzed using scanning electron microscope (SEM) during the compressive and flexural test. It is clear from all nanocomposite SEM specimens that each exhibits the characteristic features of brittle plastic deformation, including streamlined exteriors and flow cracks, demonstrating the composite's weak resistance to sustained loads or stresses implemented to the specimens.

SEM images of all the compression test specimens were somewhat similar, despite the volume fraction of glass fiber in the palmyra composite or the alkaline treatment applied to the palmyra fiber. Also, increasing the glass fiber density in the palmyra/glass fiber hybrid nanocomposites from 25% to 75% makes the composites less brittle, resulting in an occasional surface coating. Figure 13a–f shows the SEM images of the surface morphology of epoxy hybrid nanocomposites during the compressive test.

Flexural fracture through the composite is easily visible in the SEM images of the flexural test specimen, demonstrating the matrix control over the strength of the composite material. All analyzed specimens showed evidence of palmyra fiber and glass fiber deformation. This demonstrates that the matrix and fibers have excellent stress transfer with corresponding load distribution. Thermoplastic sugar starch/agar hybrid reinforced composites with seaweed/sugar palm fiber, performance comparable to fiber failure mode were noted from previous experimental results. Figure 14a–f shows the SEM images of the surface morphology of epoxy hybrid nanocomposites during the compressive test (Fig. 15).

Table 10 Flexural load value of epoxy composites with palmyra and glass fiber reinforcement

Percentage of reinforcements	Compressive yield strength	
	Untreated	Treated
GF (100%)	63.21	–
PF (100%)	42.62	52.27
EP + 75% PF + 25% GF	45.62	59.56
EP + 50% PF + 50% GF	53.21	60.24
EP + 25% PF + 75% GF	56.24	62.25

5 Conclusion

Hybrid nanocomposites were effectively prepared using alkaline (NaOH) treated palmyra and glass fiber-reinforced epoxy composites with different volume fractions.

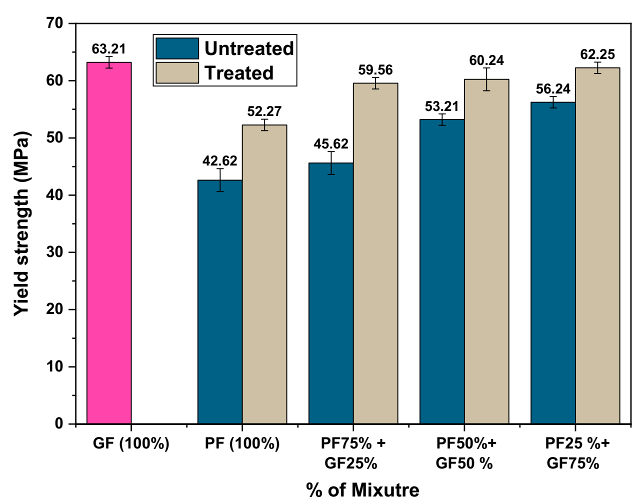

Fig. 13 Compressive yield strength epoxy composites with different volume fractions of palmyra (PF) and glass fiber (GF) reinforcement

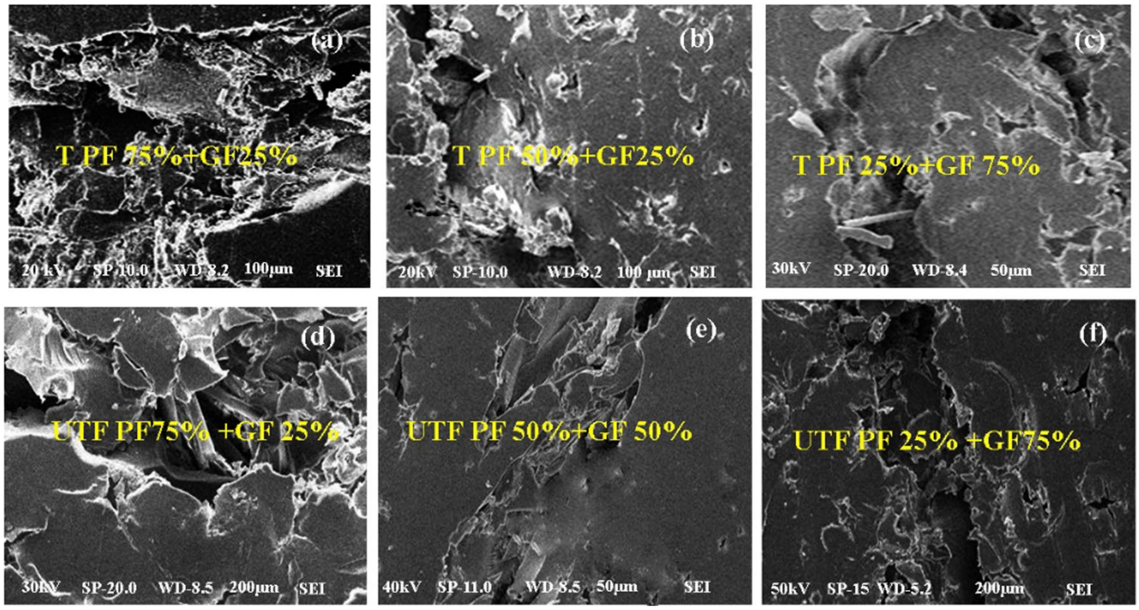

Fig. 14 **a–f** Compressive test surface morphology of (Epoxy/PF/GF) using a Scanning Electron Microscope (SEM)

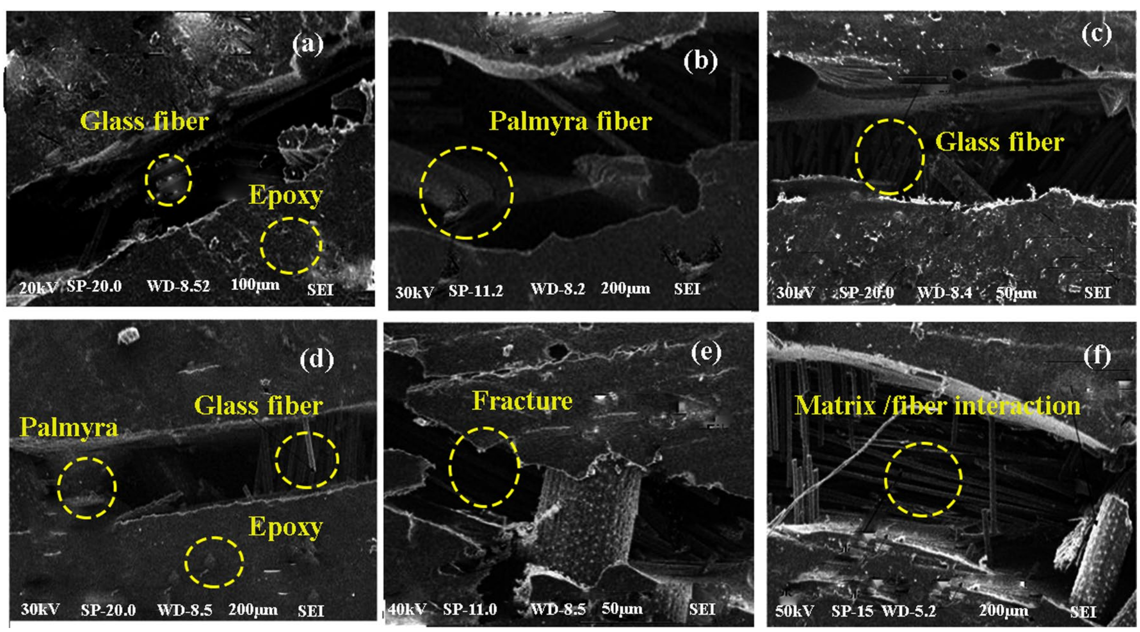

Fig. 15 **a–f** Flexural test surface morphology of (Epoxy/PF/GF) using scanning electron microscope (SEM)

Comparative analysis of flexural and compressive strength concerning their stress–strain behaviour for treated, untreated epoxy composites. The prepared hybrid nanocomposites show high flexural and compressive strength compared to untreated hybrid epoxy composites (UTPF/GF/Epoxy). With the addition of GF, the PF composite's compressive and flexural characteristics significantly improved. Additionally, it was observed that the nanocomposites' flexural and compressive characteristics improved as the GF volume fraction increased. It has a 25PF:75GF ratio that offers superior compressive (64.25 MPa) and flexural strength (75.62 MPa), particularly compared to other PF/GF/epoxy composite materials. The measured compressive and flexural properties of the 25TPF:75GF composite are supported by scanning electron microscope (SEM) analysis. Like pure GF, hybrid composites with a 25PF:75GF ratio have similar flexural and compressive properties. Moreover, the main findings of the experimental investigation outcome results proved an improved mechanical tensile, flexural, and compressive strength (detailed with stress–strain curves) as well as decreased water absorption of composite developed with Alkali-treated TPF with S-glass fiberglass reinforced epoxy composite.

Author contributions All authors contributed to the study's conception and design. Material preparation, data collection and analysis were performed by [NPS], [SS], [RV],and [RM]. The first draft of the manuscript was written by [NPS] and all authors provided language help, writing assistance and proofreading. All authors read and approved the final manuscript.

Funding The authors did not receive support from any organization for the submitted work. No funding was received to assist with the preparation of this manuscript. No funding was received for conducting this study. No funds, grants, or other support were received.

Data availability All the data required are available within the manuscript.

Declarations

Financial interest The authors have no relevant financial or non-financial interests to disclose. All authors certify that they have no affiliations with or involvement in any organization or entity with any financial or non-financial interest in the subject matter or materials discussed in this manuscript. The authors have no financial or proprietary interests in any material discussed in this article.

Conflict of interest The authors have no competing interests to declare relevant to this article's content.

Ethics approval This is an observational study. Effect of Alkaline pretreatment on Palmyra and S-Glass fiber reinforced epoxy Nanocomposites: Mechanical and water adsorption studies, Research Ethics Committee has confirmed that no ethical approval is required.

References

1. Singh MK, Tewari R, Zafar S, Rangappa SM, Siengchin S. A comprehensive review of various factors for application feasibility of natural fiber-reinforced polymer composites. Results Mater. 2023;17: 100355.
2. Mostafa NH, Ismarrubie Z, Sapuan S, Sultan M. The influence of equibiaxially fabric 440 prestressing on the flexural performance of woven E-glass/polyester-reinforced 441 composites. J Compos Mater. 2016;50:3385–93.
3. Safri SNA, Sultan MTH, Jawaid M, Jayakrishna K. Impact behaviour of hybrid composites for structural applications: a review. Compos B Eng. 2018;133:112–21.
4. Andrew JJ, Dhakal HN. Sustainable biobased composites for advanced applications: recent trends and future opportunities—a critical review. Compos C Open Access. 2022;7:100220.
5. Ramesh M. Kenaf (*Hibiscus cannabinus* L.) fiber-based biomaterials: a review on processing and properties. Prog Mater Sci. 2016;78–79:1–92.
6. Kisiel M, Mossety-Leszczak B. Development in liquid crystalline epoxy resins and composites—a review. Eur Polym J. 2020;124: 109507.
7. Dagdag O, Safi Z, Hsissou R, Erramli H, El Bouchti M, Wazzan N, Guo L, Verma C, Ebenso EE, El Harfi A. Epoxy pre-polymers as new and effective materials for corrosion inhibition of carbon steel in acidic medium: computational and experimental studies. Sci Rep. 2019;9:11715.
8. Wan J, Zhao J, Zhang X, Fan H, Zhang J, Hu D, et al. Epoxy thermosets and materials derived from bio-based monomeric phenols: transformations and performances. Progr Polym Sci. 2020;108:101287.
9. Wan J, Zhao J, Zhang X, Fan H, Zhang J, Hu D, Jin P, Wang D-Y. Epoxy thermosets and materials derived from bio-based monomeric phenols: transformations and performances. Prog Polym Sci. 2020;108: 101287.
10. Zhang H, Li W, Xu J, Shang S, Song Z. Synthesis and characterization of bio-based epoxy thermosets using rosin-based epoxy monomer. Iran Polymer J. 2021;30:643–54.
11. Ozgul EO, Ozkul MH. Effects of epoxy, hardener, and diluent types on the hardened state properties of epoxy mortars. Constr Build Mater. 2018;187:360–70.
12. Krishna KG, Divakar C, Venkatesh K, et al. Bulk temperature estimation during wear of a polymer composite pin. Wear. 2010;268:346–51.
13. Hussain M, Gupta A, Kumar P, Hussain MI, Das AK. Experimental study and statistical analysis of bending titanium alloy sheet with continuous wave fiber laser. Archiv Civil Mech Eng. 2022;22:110.
14. Sanjeevi S, Shanmugam V, Kumar S, Ganesan V, Sas G, Johnson DJ, Shanmugam M, Ayyanar A, Naresh K, Oisik REN. Effects of water absorption on the mechanical properties of hybrid natural fiber/phenol formaldehyde composites. Sci Rep. 2021;11:13385.
15. Evans PD, Owen NL, Schmid S, Webster RD. Weathering and photostability of benzoylated wood. Polym Degrad Stab. 2002;76:291–303.
16. Fartini M, Majid MA, Ridzuan M, Amin N, Gibson A. Compressive properties of Napier (*Pennisetum purpureum*) filled polyester composites. Plast Rubber Compos. 2016;45:136–41.
17. Vasudevan A, Kumar BN, Depoures MV, Maridurai T, Mohanavel V. Tensile and flexural behaviour of glass fiber reinforced plastic–aluminium hybrid laminate manufactured by vacuum resin transfer moulding technique (VARTM). Mater Today Proc. 2021;37:2132–40.
18. Raju JSN, Depoures MV, Shariff JA, Chakravarthy S. Characterization of natural cellulosic fibers from stem of *Symphirema involucratum* plant. J Nat Fibers. 2022;19(13):5355–70.
19. Velmurugan R, Manikandan V. Mechanical properties of palmyra/glass fiber hybrid composites. Compos A Appl Sci Manuf. 2007;38(10):2216–26.
20. Sherwani SFK, et al. Mechanical properties of sugar palm (*Arenga innata* Wurmb. Merr)/glass fiber-reinforced poly(lactic acid) hybrid composites for potential use in motorcycle components. Polymers. 2021;13:3061. https://doi.org/10.3390/polym13183061.
21. Bekele AE, et al. Study of the effects of alkali treatment and fiber orientation on mechanical properties of enset/sisal polymer hybrid composite. J Compos Sci. 2023;7:37. https://doi.org/10.3390/jcs7010037.
22. Kong F, et al. On the vibrations of the electrorheological sandwich disk with composite face sheets considering pre and post-yield regions. Thin-Walled Struct. 2022;179:109631. https://doi.org/10.1016/j.tws.2022.109631.
23. Arshid E, et al. Porosity-dependent vibration analysis of FG microplates embedded by polymeric nanocomposite patches considering hygrothermal effect via an innovative plate theory. Eng Comp. 2022;38:4051–72. https://doi.org/10.1007/s00366-021-01382-y.

24. Garg A, et al. Machine learning models for predicting the compressive strength of concrete containing nano-silica. Comput Concrete. 2022;30(1):33–42. https://doi.org/10.12989/cac.2022.30.1.033.
25. Djilali N, et al. Large cylindrical deflection analysis of FG carbon nanotube-reinforced plates in thermal environment using a simple integral HSDT. Steel Compos Struct. 2022;42(6):779–89. https://doi.org/10.12989/scs.2022.42.6.779.
26. Huang Y, et al. Static stability analysis of carbon nanotube reinforced polymeric composite doubly curved micro-shell panels. Archiv Civil Mech Eng. 2021;21:139. https://doi.org/10.1007/s43452-021-00291-7.
27. Zerrouki R, et al. Effect of nonlinear FG-CNT distribution on mechanical properties of functionally graded nano-composite beam. Struct Eng Mech. 2021;78(2):117–24. https://doi.org/10.12989/sem.2021.78.2.117.
28. Bendenia N, et al. Deflections, stresses and free vibration studies of FG-CNT reinforced sandwich plates resting on Pasternak elastic foundation. Comput Concrete. 2020;26(3):213–26. https://doi.org/10.12989/cac.2020.26.3.213.
29. Fouad F, et al. Stability and dynamic analyses of SW-CNT reinforced concrete beam resting on elastic-foundation. Comput Concrete. 2020;25(6):485–95. https://doi.org/10.12989/cac.2020.25.6.485.
30. Al-Furjan MSH, et al. A computational framework for propagated waves in a sandwich doubly curved nanocomposite panel. Eng Comput. 2022;38:1679–96.
31. Al-Furjan MSH, et al. Frequency simulation of viscoelastic multi-phase reinforced fully symmetric systems. Eng Comput. 2022;38:3725–41.
32. Al-Furjan MSH, et al. On the vibrations of the imperfect sandwich higher-order disk with a lactic core using generalize differential quadrature method. Compos Struct. 2021;257:113150.
33. Heidari F, et al. On the mechanics of nanocomposites reinforced by wavy/defected/aggregated nanotubes. Steel Compos Struct. 2021;38:533–45. https://doi.org/10.12989/scs.2021.38.5.533.
34. Al-Furjan MSH, et al. Non-polynomial framework for stress and strain response of the FG-GPLRC disk using three-dimensional refined higher-order theory. Eng Struct. 2021;228(1):111496.
35. Thomason J. An overview of some scaling issues in the sample preparation and data interpretation of the micro bond test for fiber–matrix interface characterization. Polym Testing. 2022;111:107591.
36. Hasan KMF, Horváth PG, Kóczán Z, Alpár T. Thermo-mechanical properties of pretreated coir fiber and fibrous chips reinforced multilayered composites. Sci Rep. 2021. https://doi.org/10.1038/s41598-021-83140-0.
37. Paul SA, Boudenne A, Ibos L, Candau Y, Joseph K, Thomas S. Effect of fiber loading and chemical treatments on thermophysical properties of banana fiber/polypropylene commingled composite materials. Compos A Appl Sci Manuf. 2008;39:1582–8.